Appendix B: Comparison between Fixed angles and range angles systems in the case of Nickel

This section presents the comparison of the fixed angles using Au cathode template and range angles systems using Cu cathode template. The two configurations have been presented in Subsection 2.1.1. Only Ni systems have been studied. The difference between those two samples configuration still have to be investigated in more detail but some information may already be derived from this single comparison. The investigated Au cathode Ni CNWs network was electro-deposited in a template with α angle encompassed between 20° and 25° with respect to the normal of the PC film surface. The potential used was -1.1 V. It is the same value than for the Ni sample created in Cu cathode template. The Cu cathode Ni CNWs netork used for comparison has been presented in Subsection 2.1.2. It presents an uniform distribution for the NWs orientation in the range $-\alpha_{max} \leq \alpha \leq \alpha_{max}$ with respect to the normal of the PC film surface.

Figure 74 compares the AMR curves of Ni 40nm CNWs networks deposit in Cu cathode template (black) and in Au cathode template (red). The effect looks stronger in the Cu cathode sample, in comparison to the Au cathode one. However, there is no reason to have a decrease of the AMR effect, as it is the same material. The configuration being different, the values of R_{IP} and R_{OOP} have different meanings. One can observe that the saturation seems easier in the cu cathode template in both direction.

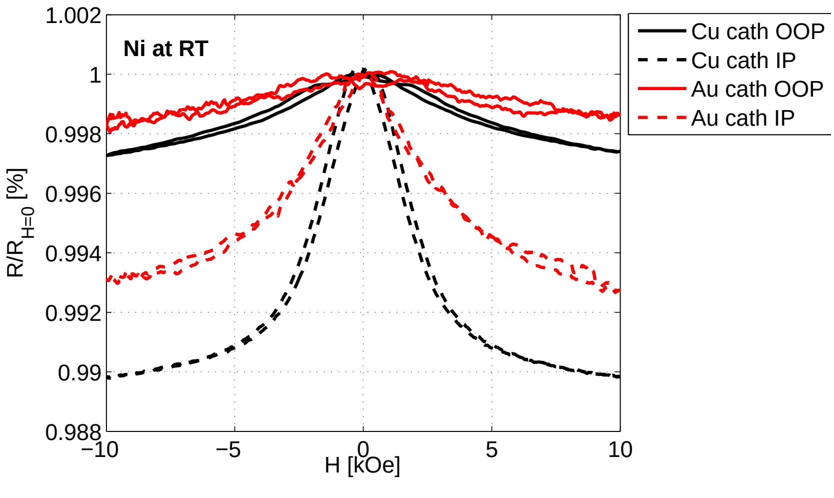

Figure 74: Comparison of the room temperature anisotropic magnetoresistance (AMR) curves obtained for Ni 40nm CNWs networks deposited in Cu cathode template (black) and Au cathode template (red). Continuous lines correspond to the measurements obtained when applying the external field in the OOP direction and the dashed lines correspond to the measurements obtained when applying the external field in the IP direction.

Similarly to the model developed for the Cu cathode samples (See subsection 3.4.1), a model can be developed for the Au cathode samples. The azimuthal angle β will be supposed equal to $45°$. The angles between the NWs and the OOP direction are in the range of $20° \leq \alpha \leq 25°$ ($\frac{\pi}{9} \leq \alpha \leq \frac{5\pi}{36}$).

First, supposing only one value of the α angle ($\alpha = 20°$ or $\alpha = 25°$), on can easily derives:

$$\frac{\rho_{\perp}^{OOP}}{\rho_{\parallel}} = \frac{1}{1-\cos^2(\alpha)}(\frac{\rho_{OOP}}{\rho_{\parallel}} - \cos^2(\alpha)) \tag{85}$$

$$\frac{\rho_{\perp}^{IP}}{\rho_{\parallel}} = \frac{1}{1-\cos^2(\theta)}(\frac{\rho_{IP}}{\rho_{\parallel}} - \cos^2(\theta)) \tag{86}$$

With $\cos(\theta) = \cos(\beta)\sin(\alpha) = \frac{1}{\sqrt{2}}\sin(\alpha)$:

$$\frac{\rho_{\perp}^{IP}}{\rho_{\parallel}} = \frac{1}{1-\frac{1}{2}\sin^2(\alpha)}(\frac{\rho_{IP}}{\rho_{\parallel}} - \frac{1}{2}\sin^2(\alpha)) \tag{87}$$

Because the configuration where the magnetisation is perpendicular to the NWs axis is independent of the direction of the magnetic field one can suppose that $\frac{\rho_{\perp}^{OOP}}{\rho_{\parallel}} = \frac{\rho_{\perp}^{IP}}{\rho_{\parallel}}$. Therefore:

$$\frac{1}{1-\frac{1}{2}\sin^2(\alpha)}(\frac{\rho_{IP}}{\rho_{\parallel}} - \frac{1}{2}\sin^2(\alpha)) = \frac{1}{1-\cos^2(\alpha)}(\frac{\rho_{OOP}}{\rho_{\parallel}} - \cos^2(\alpha)) \tag{88}$$

$$\frac{\rho_{IP}}{\rho_{\parallel}} = \frac{1-\frac{1}{2}\sin^2(\alpha)}{1-\cos^2(\alpha)}(\frac{\rho_{OOP}}{\rho_{\parallel}} - \cos^2(\alpha)) + \frac{1}{2}\sin^2(\alpha) \tag{89}$$

Now if one considers that α can vary between 20° and 25°, one can write:

$$\bar{\rho}_{OOP} = \frac{1}{L}\int_{\frac{\pi}{9}}^{\frac{5\pi}{36}} \rho_{\perp} + (\rho_{\parallel} - \rho_{\perp})\cos^2(\theta)\ \mathrm{d}\theta \tag{90}$$

With $L = \frac{\pi}{9} - \frac{5\pi}{36} = \frac{\pi}{36}$. If one integrates the expression, it gives:

$$\bar{\rho}_{OOP} = K_{OOP}^{+}\rho_{\parallel} + K_{OOP}^{-}\rho_{\perp} \tag{91}$$

With $K_{OOP}^{+} = \frac{1}{2} + \frac{1}{4\frac{\pi}{36}}(\sin(2\frac{5\pi}{36}) - sin(2\frac{\pi}{9})))$ and $K_{OOP}^{-} = \frac{1}{2} - \frac{1}{4\frac{\pi}{36}}(\sin(2\frac{5\pi}{36}) - sin(2\frac{\pi}{9})))$.

Similarly, one can writes:

$$\bar{\rho}_{IP} = \frac{1}{L}\int_{\theta_1}^{\theta_2} \rho_{\perp} + (\rho_{\parallel} - \rho_{\perp})\cos^2(\theta)\ \mathrm{d}\theta \tag{92}$$

With $\cos(\theta_1) = \cos(\beta)\sin(\frac{\pi}{9}) = \frac{1}{\sqrt{2}}\sin(\frac{\pi}{9})$, $\cos(\theta_2) = \cos(\beta)\sin(\frac{5\pi}{36}) = \frac{1}{\sqrt{2}}\sin(\frac{5\pi}{36})$ and $L = \theta_2 - \theta_1$. It gives:

$$\bar{\rho}_{IP} = K_{IP}^{+}\rho_{\parallel} + K_{IP}^{-}\rho_{\perp} \tag{93}$$

With $K_{OOP}^{+} = \frac{1}{2} + \frac{1}{4L}(\sin(2\theta_2) - sin(2\theta_1)))$ and $K_{OOP}^{-} = \frac{1}{2} - \frac{1}{4L}(\sin(2\theta_2) - sin(2\theta_1)))$.

One can then derive:

$$\frac{\rho_{\perp}^{OOP}}{\rho_{\parallel}} = \frac{1}{K_{OOP}^{-}}(\frac{\bar{\rho}_{OOP}}{\rho_{\parallel}} - K_{OOP}^{+}) \tag{94}$$

$$\frac{\rho_{\perp}^{IP}}{\rho_{\parallel}} = \frac{1}{K_{IP}^{-}}(\frac{\bar{\rho}_{IP}}{\rho_{\parallel}} - K_{IP}^{+}) \tag{95}$$

Using the hypotesis that $\frac{\rho_{\perp}^{OOP}}{\rho_{\|}} = \frac{\rho_{\perp}^{IP}}{\rho_{\|}}$:

$$\frac{\bar{\rho}_{IP}}{\rho_{\|}} = \frac{K_{IP}^{-}}{K_{OOP}^{-}} \frac{\bar{\rho}_{OOP}}{\rho_{\|}} + \frac{1}{K_{OOP}^{-}}(K_{OOP}^{-}K_{IP}^{+} - K_{OOP}^{+}K_{IP}^{-}) \tag{96}$$

Figure 75 shows the comparison between the model just derived for Au cathode samples (red) and the model developed for Cu cathode samples (black) along with the experimental results for Ni. Note that in the case of the model developed for Au cathode samples, the center dashed lines correspond to an angle varying from 20° to 25° and the extreme dash line corresponds to $\alpha = 20°$ and $\alpha = 25°$. The experimental data fits very well the $\alpha = 25°$ curve.

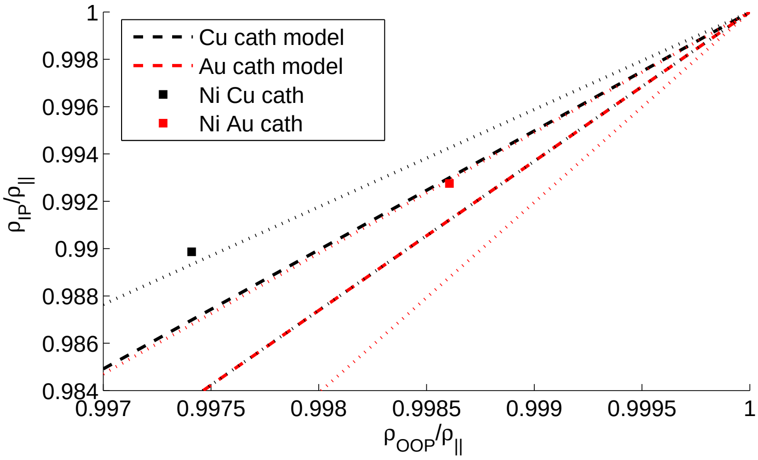

Figure 75: Comparison of the mathematical model and experimental results obtained for Ni 40nm CNWs networks deposited in Cu cathode template (black) and Au cathode template (red). Dashed black line correspond to the model for range α angle with $\beta = \alpha_{max} = \frac{\pi}{4}$ and the black dotted lines take into account the $\pm 5°$ standard deviation. Dashed red line correspond to the model of α angle varying between 20° and 25°, while dotted red line consider either $\alpha = 20°$ and $\alpha = 25°$.

Table 19 provides the values of $\frac{\rho_{\perp}^{OOP}}{\rho_{\|}}$, $\frac{\rho_{\perp}^{IP}}{\rho_{\|}}$ and the mean AMR value with its standard deviation for the Ni CNWs network deposited in a Au cathode template, all calculated using a range of angles varying between $\alpha = 20°$ and $\alpha = 25°$. The AMR of the Ni CNWs network with Cu cathode is provided for comparison. The same order of AMR effect magnitude is found. If one only uses the measurements made when increasing the external magnetic field in the IP direction, which may be more accurate due to a bigger variation of the resistance, one obtains 1.1%. More measurements have to be made in Au cathode samples in the future to highlights the effect of this other configuration.

Table 19: $\frac{\rho_{\perp}^{OOP}}{\rho_{\|}}$, $\frac{\rho_{\perp}^{IP}}{\rho_{\|}}$, the AMR mean value between IP and OOP calculation with the standard deviation, all calculated using a angle varying between $\alpha = 20°$ and $\alpha = 25°$, and the AMR of the Ni CNWs network with Cu cathode for comparison.

$\frac{\rho_{\perp}^{OOP}}{\rho_{\|}}$	$\frac{\rho_{\perp}^{IP}}{\rho_{\|}}$	AMR [%]	AMR Cu Cathode
0.9824	0.9891	1.44 ±0.48	1.16